JACS
JOURNAL OF THE AMERICAN CHEMICAL SOCIETY
Article
pubs.acs.org/JACS

Nonadiabatic Dynamics of Charge Transfer and Singlet Fission at the Pentacene/C_{60} Interface

Alexey V. Akimov[†,‡] and Oleg V. Prezhdo*[,†]

[†]Department of Chemistry, University of Rochester, Rochester, New York 14627, United States
[‡]Department of Chemistry, Brookhaven National Laboratory, Upton, New York 11973, United States

ABSTRACT: Charge carrier multiplication in organic heterojunction systems, a process known as singlet fission (SF), holds promise for development of solar cells with enhanced photon-to-electron yields, and therefore it is of substantial fundamental interest. The efficiency of photovoltaic devices based on this principle is determined by complex dynamics involving key electronic states coupled to particular nuclear motions. Extensive experimental and theoretical studies are dedicated to this topic, generating multiple opinions on the nature of such states and motions, their properties, and mechanisms of the competing processes, including electron−phonon relaxation, SF, and charge separation. Using nonadiabatic molecular dynamics, we identify the key steps and mechanisms involved in the SF and subsequent charge separation, and build a comprehensive kinetic scheme that is consistent with the existing experimental and theoretical results. The ensuing model provides time scales that are in excellent agreement with the experimental observations. We demonstrate that SF competes with the traditional photoinduced electron transfer between pentacene and C_{60}. Efficient SF relies on the presence of intermediate dark states within the pentacene subsystem. Having multiexciton and charge transfer character, these states play critical roles in the dynamics, and should be considered explicitly when explaining the entire process from the photoexcitation to the final charge separation.

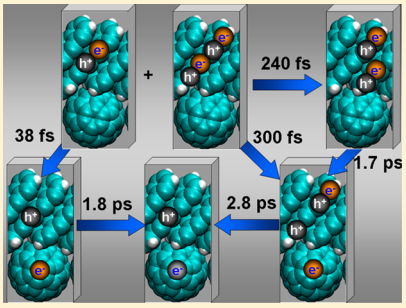

1. INTRODUCTION

Efficient conversion of solar energy into electric current (photovoltaic cell) or chemical transformations (photocatalytic cell) constitutes one of the most challenging and worthwhile goals in contemporary science and engineering.[1−4] A wide range of studies, both experimental[5−12] and theoretical,[10,13−24] focus on developing new types of solar cells, their optimization, and understanding the details of the underlying physical processes. The maximal theoretical efficiency of the conventional solar cells, determined by the thermodynamic factors, is estimated to be ca. 31%.[25] This limit arises from the fact that the energy of adsorbed photons, in excess of the lowest excitation energy in a material, is transformed into thermal motion of atoms instead of creating charges. It has been found, however, that this limit can be overcome if the excess energy is channeled into excitation of additional electrons. One absorbed photon then can produce two or more pairs of charge carriers. This process is known as impact ionization in bulk semiconductors,[26,27] multiple exciton generation (MEG) in quantum dots[12−15,19−25] and carbon nanotubes,[28−30] and singlet fission (SF) in organic molecular systems.[6,11−13,31−45]

Crystalline pentacene is one of the better-studied materials exhibiting SF.[32,43,44,46,47] It has been shown that the process involves an intermediate doubly excited state, a multiexciton (ME). Subsequent transformation of this state produces two coupled triplet excitons, localized on different parts of the molecular system, thus creating two excited electrons per one absorbed photon (Figure 1). Recent time-resolved two-photon photoemission studies[32] have confirmed the existence of the ME state in pentacene/C_{60}.

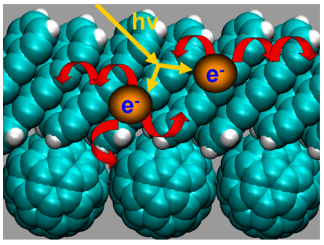

Figure 1. Singlet fission and charge transfer processes in a pentacene/C_{60} solar cell. Photon absorption creates a superposition of singly and doubly excited configurations. The ensuing electron−nuclear dynamics can lead to singlet fission and charge separation by electron transfer from pentacene to C_{60}.

Time-resolved experimental data can be used to construct a kinetic model for the excited state dynamics leading to SF. A more detailed description of the dynamics requires theoretical investigations, which can characterize the electronic origin of the states involved and determine the mechanisms of their transformation. The state properties and transformation mechanisms must be consistent with the observed excitation process and charge transfer rates, which provide constraints and tests for the theory. Severe limitations on the theoretical studies of such systems, and especially the processes involving ME

Received: November 19, 2013
Published: January 7, 2014

   dx.doi.org/10.1021/ja411800n | J. Am. Chem. Soc. 2014, 136, 1599−1608

configurations, arise because of the extreme complexity of the problem. On the one hand, high-level static electronic structure calculations of systems exhibiting SFs, including multiconfigurational treatment of the wave functions, have been performed.[43,44,48] In such approaches, the electron transfer (ET) rates between select states can be estimated using the Marcus theory, Fermi golden rule, and Landau−Zener expressions. Similar in spirit, the density matrix method combined with an ab initio parametrization has been successfully employed to study SF in several organic materials.[33] On the other hand, direct dynamical simulation of the nonadiabatic electron and energy transfer has been carried out for complex systems, however with a restriction to the singly excited configurations.[49−51] ME states have been included in such simulation for systems, such as inorganic quantum dots, in which the independent particle, band structure representation provides a good zeroth-order approximation.[21,52] Theoretical study of the SF and ET processes in the pentacene/C_{60} system is challenging because both the direct dynamical simulation and the multiconfigurational treatment of the wave function are necessary, pushing the limits of currently available computational techniques.

In this work, we build a model for the description of dynamics of the states involved in the SF, electron−phonon relaxation, and ET processes in the pentacene/C_{60} heterojunction. Our approach is based on a combination of the nonadiabatic ab initio molecular dynamics technique[53,54] and the available computational[43,44,48,55] and experimental information.[32,40,43,45−47,56−58] Because of the complexity of the problem, some of the experimental and theoretical studies show inconsistent and even contradictory results and predictions. Depending on the energy of the intermediate charge transfer states, different mechanisms of charge transfer and SF may be proposed. As suggested by Yi et al.,[48] the energy of the state that corresponds to transfer of an electron from pentacene to C_{60} lies 1.2−1.4 eV above the ground electronic state. On the contrary, as suggested by the experimental studies of Rao et al.,[45] the energy of the charge transfer state is notably lower, ca. 0.5 eV, in agreement with the open circuit voltage of pentacene/C_{60} solar cells. The energies of the excited charge transfer states are estimated at 1.15 eV[57] and 1.31 eV[58] above the energy of the lowest charge transfer state. Whether or not the charge transfer states are important for the photoinduced dynamics depends crucially on the location of their energies relative to the energies of the excitonic states.

Another set of inconsistent results concerns the mechanism and time scale of SF. According to Thorsmolle et al.,[46,47] Jundt et al.,[56] and Wilson et al.,[42] singlet fission is a direct $S_1 \rightarrow 2\ T_1$ process. In comparison, as suggested by the recent ab initio calculations of Zimmerman et al.[43,44] and later experimental studies of Chan et al.,[32] the process involves an optically inactive doubly excited state that mediates the transition. The triplet generation rates vary by an order of magnitude, from 80 fs, as reported by Jundt et al.[56] and Wilson et al.,[42] to 700 and 900 fs as reported by Thorsmolle et al.[46,47] and Chan et al.,[32] respectively. This variation may be attributed to the differences in proposed SF mechanisms.

As the consequence of the different views on the mechanism of the coupled triplet pair production, the interpretations of the experiments vary. In the experiment carried out by Thorsmolle et al.,[46,47] doping of pentacene crystals with C_{60} leads to quenching of the triplet state. The researchers conclude that the S_1 state is the main source of the produced triplets. On the contrary, the experiments by Chan et al.[32] indicate that the ME state is a precursor of the coupled triplet pair, and that the ME state does not arise from the decay of the S_1 state. Although fullerene is present in the system and serves as the ultimate electron collector, it does not strongly affect the charge carrier multiplication.

Our approach aims to conciliate the contradictions as much as possible, to provide mechanistic insights into the underlying dynamical processes, and to establish a theoretical framework for elucidating the SF and charge transfer processes in the pentacene/C_{60} system. In particular, with the regard of the examples discussed above, the following questions need resolving: (a) What is the energy of the lowest energy charge transfer state (CT_0) in the pentacene/C_{60} system? Are the excited charge transfer states (CT_1, CT_2) important for the photoinduced dynamics? (b) What is the SF mechanism? Is the intermediate doubly excited state (ME) important? Is the ME state produced by decay of the S_1 state? Is the direct $S_1 \rightarrow 2T_1$ transition important? (c) What are the time scales of the involved processes? (d) Would the quenching of S_1 via charge transfer to C_{60} preclude SF?

2. METHODS

Constrained by the complexity of the problem and by the goal to perform time-domain atomistic simulations, we adopt a multistep procedure to develop the theoretical model. We identify the key electronic states involved in photoinduced dynamics on the basis of the experimental results and high-level static quantum-mechanical calculations. The nonadiabatic coupling matrix elements between the states are computed with ab initio density functional theory (DFT). The time-domain simulations of the photoinduced dynamics in the pentacene/C_{60} system are performed using a mixed quantum-classical technique, combining time-domain DFT and fewest switches surface hopping.

2.1. Ab Initio Molecular Dynamics. All quantum-mechanical and electron−nuclear dynamics calculations are performed with the Quantum Espresso program,[59] which utilizes plane waves and the ultrasoft pseudopotential generated within the PBE generalized gradient DFT functional.[60,61] The size of the plane wave basis is chosen to satisfy the 40 Ry energy and 400 Ry charge density cutoffs. The dispersion correction was included via the semiempirical London terms (DFT-D).[62,63] The initially optimized structure of the pentacene/C_{60} system, containing two pentacene molecules and one C_{60} molecule per simulation cell (Figure 1), is equilibrated for 1 ps using the 1.0 fs time step. The system geometry changed little during equilibration, indicating that the 1 ps equilibration time is sufficient. The following 2 ps of molecular dynamics simulation is used for analysis. The geometry of the pentacene−fullerene multilayer heterojunction used in this work closely resembles that proposed by the atomistic MD simulations.[64] Similarly, the vertical orientation of the pentacene molecules with respect to the fullerene layer surface is adopted. For computational simplicity, we include only a minimal number of pentacene molecules, two. This model is adequate for capturing dynamics of the ME and charge transfer states. At the same time, we anticipate that using more sophisticated models of the heterojunction will not change the qualitative (and even quantitative) picture of the quantum dynamics drastically. The Nose−Hoover thermostat[65−68] with the temperature of 300 K is employed to perform simulations in the NVT ensemble, corresponding to the experimental conditions. Twenty initial conditions for the nonadiabatic molecular dynamics simulations are sampled from the 2 ps NVT trajectory. 200 stochastic surface hopping trajectories are computed for each nuclear initial condition, resulting in 4000 total electronic-nuclear evolutions.

2.2. Nonadiabatic Molecular Dynamics. To model the SF and ET processes, it is crucial to employ a methodology capable of describing transitions between electronic states. Nonadiabatic

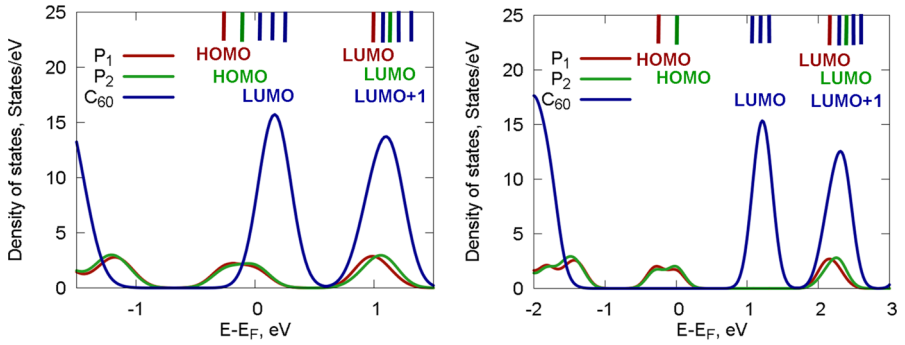

Figure 2. Contributions to the density of states from C_{60} and the two pentacenes, P_1 and P_2, forming the simulation cell (Figure 1). Parts (a) and (b) show the data obtained using the PBE and PBE0 functionals, respectively. The colored vertical bars indicate the (quasi)degenerate energy levels composing each MO band.

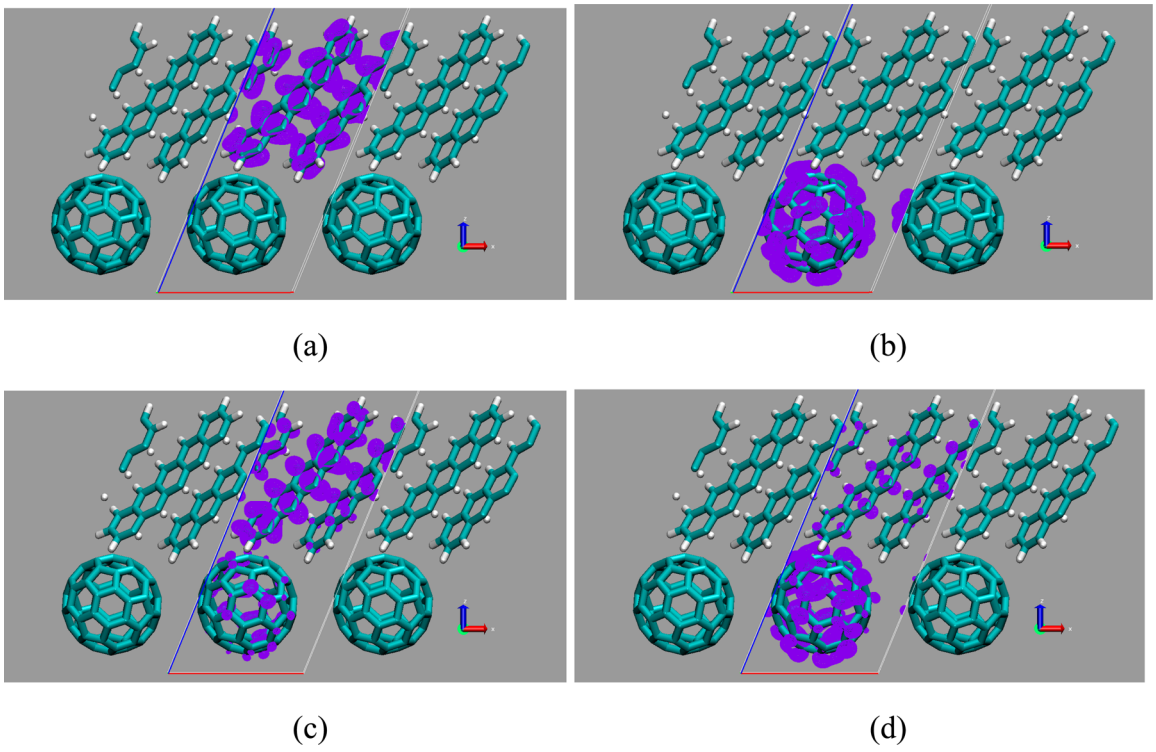

Figure 3. Charge density of the frontier KS orbitals: one of the two quasi-degenerate HOMO states, localized on pentacene (a); one of the three quasi-degenerate LUMO states, localized on C_{60} (b); LUMO of pentacenes (c); and LUMO+1 of C_{60} (d). The orbital tails extend onto the complementary subsystem and ensure efficient donor−acceptor coupling.

molecular dynamics and, in particular, trajectory surface hopping[53,54] provide an efficient method that is capable of describing electronic transitions in large systems. In this work, we utilize the classical path approximation combined with the fewest switches surface hopping, as implemented in the PYXAID package.[69] The time-dependent KS equations are solved along a precomputed trajectory, $R(t)$, that is, the 2 ps NVT trajectory discussed in section 2.1. The probability of electronic transitions between basis states $|i\rangle$ and $|j\rangle$ is determined by the time-dependent amplitudes $\{c_i(t)\}$ in the basis set expansion of the wave function $|\Psi(t,R)\rangle = \sum_i c_i(t)|i(R)\rangle$, and by the magnitude of the nonadiabatic coupling $d_{ij} = \langle i|(\mathrm{d}/\mathrm{d}t)|j\rangle$. A detailed description of the algorithm and discussion of its capabilities and limitations can be found elsewhere.[4,53,69−73] Unlike several other formulations, based on semiempirical Hamiltonians,[70,74−76] we utilize an electronic Hamiltonian based on the DFT. The many-electron configurations expressed using Slater determinants are built from the one-electron Kohn−Sham (KS) orbitals. The nonadiabatic couplings between the many-electron configurations can be expressed in terms of the nonadiabatic couplings between the KS orbitals.[49,69] They are computed numerically using the approximation.[77]

The electronic basis states $\{|i\rangle\}$ can be defined in a variety of ways. In this work, we utilize Slater determinants constructed from the Kohn−Sham orbitals[49,69] and introduce corrections based on the more rigorous electronic structure calculations[43,44,48,78] or on experimental data.[32,40,43,45−47,56−58] The representation provides substantial computational savings and has been successfully used in various applications involving large systems[50,51,79−82] or a large number of excited states.[21,52] Currently, we consider the electronic configurations involving several frontier KS orbitals and 4 active electrons. A detailed discussion of the basis states and their energies is presented in following sections. Experiments provide direct information on the excited state energies, and electronic structure approaches characterize the orbital origin of the excitations. In addition to this information, a time-domain description of the SF and ET processes requires

dx.doi.org/10.1021/ja411800n | J. Am. Chem. Soc. 2014, 136, 1599−1608

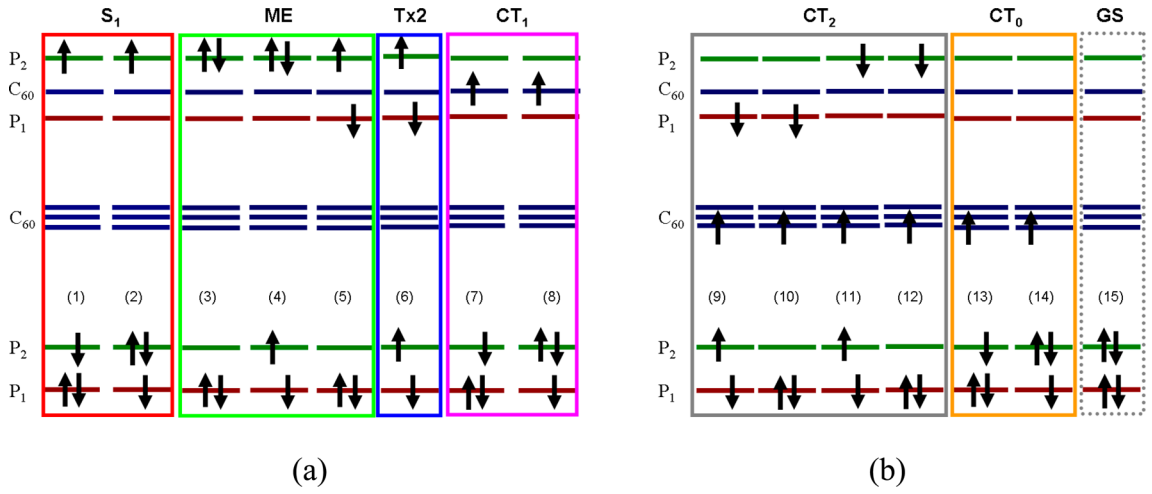

Figure 4. Schematic representation of configurations used for description of the singlet fission and charge transfer processes.

knowledge of the nonadiabatic coupling, which are obtained in the present calculations as functions of time. Because the experimental SF yields are significantly lower in dimers than in crystals,[83] our periodic model is particularly relevant for solar energy applications as compared to models based on finite systems.

3. RESULTS AND DISCUSSION

3.1. Properties of One-Electron Orbitals. Projected density of states (pDOS), obtained by projecting the total density of states onto atomic orbitals, allows one to understand which one-electron transitions may be dominant in description of many-electron excited states. The pDOS presented in Figure 2 are computed at the PBE and PBE0 levels of theory, and characterize molecular orbital (MO) localization on C_{60} and each of the two pentacenes.

The PBE calculations show a very small HOMO−LUMO gap, a well-known shortcoming of pure density functionals (Figure 2a).[84−89] Yet, the relative position of the occupied, valence band (VB) energy levels and unoccupied, conduction band (CB) states is similar to that obtained with the more accurate PBE0 method (Figure 2b). The similarity of the PBE and PBE0 band structures refers to the order of occupied and vacant orbitals, which is the same in both cases. The gaps are different in the two cases, and the PBE gap is corrected on the basis of the PBE0 result with the "scissor operator" technique. Note that PBE0 calculations with periodic systems are orders of magnitude more expensive than PBE calculations, while the use of explicitly correlated methods and many-body perturbation theory is even more time-consuming.

The two highest occupied orbitals are localized on the two pentacenes (Figure 3a). The LUMO is composed of three quasi-degenerate states localized on the C_{60} fragment (Figure 3b). The shape of the charge density of these three levels mimics that of the three hydrogen-like P states that arise from the particle-on-a-sphere treatment of electron in C_{60}, similarly to the particle-in-a-spherical-well model of quantum dots.[18] Other unoccupied MOs relevant to the photoexcitation, SF, and charge transfer dynamics in this system include the unoccupied orbitals localized on the pentacene fragments (Figure 3c) and the LUMO+1 levels of C_{60} (Figure 3d). The latter are triply degenerate and are energetically close to the LUMO levels of pentacene.

3.2. Many-Electron States. To model the excited-state dynamics in the pentacene/C_{60} system, we consider a basis of singly and doubly excited Slater determinants, as illustrated in Figure 4. The construction and classification of the determinants is based on the localization of the occupied KS orbitals and on the number of excited electrons. Within this zeroeth-order adiabatic framework, the nonadiabatic couplings d_{ij} between states differing by more than one occupied orbital are zero.[49] Thus, only configurations that are related to each other by a single electron transition are coupled. For example, configurations 3 and 4 of the ME type (Figure 4a) are not coupled to the ground-state configuration 15 (Figure 4b), while they are coupled to configurations 1 and 2 of the S_1 type (Figure 4a) and to each other.

The definition of the states in Figure 4 is based on the existing theoretical and experimental knowledge. According to the previous studies, it is known that the optically active singly excited states (S_1, Figure 4a) can be described approximately by a transfer of one electron from HOMO to LUMO of the pentacenes.[43] The doubly excited state of a pentacene dimer (ME) involves configurations with two electrons promoted from HOMO to LUMO within the pentacene subsystem, as exemplified by configurations 3−5 in Figure 4a.[43] The dynamics simulation considers the doubly excited configurations individually. During the analysis, we group them under the ME label, because they all involve excitation of multiple electrons, are optically dark, and are intermediates for SF in the pentacene subsystem and ET between pentacene and C_{60}.

The state corresponding to a pair of correlated triplets (Tx2) involves the excitation of two electrons, similarly to the ME configurations, but each of these two electrons is excited within the same molecule. This situation is exemplified by configuration 6 in Figure 4a. Note that the direct transition between determinants 3 and 6 is forbidden in the single-particle description, because it would require simultaneous transition of more than one electron. It can happen with the help of configurations 4 and 5 (Figure 5). We want to emphasize that the Tx2 state has the overall singlet spin-multiplicity and is not to be confused with the isolated triplet state. Thus, the mechanisms of nonadiabatic transitions are not complicated by possible spin-flip processes, which would need special treatment.

The lowest-energy state involving ET between pentacene and C_{60} (CT_0, Figure 4b, configurations 13 and 14) is described as the direct product of the ground state of the C_{60} radical anion and the ground state of the pentacene radical cation, as

dx.doi.org/10.1021/ja411800n | J. Am. Chem. Soc. 2014, 136, 1599−1608

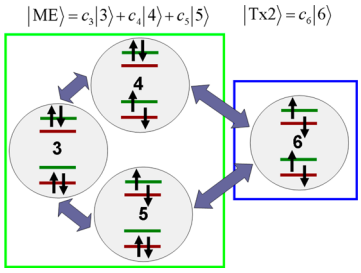

Figure 5. Schematic representation of the coupling between the ME = {3,4,5} and Tx2 = {6} states illustrated in Figure 4. The 3 → 6 transition cannot occur directly; it is mediated by states 4 and 5.

discussed elsewhere.[48] The first excited charger transfer state (CT_1) is constructed as the direct product of the first excited state of the C_{60} anion and the ground state of the pentacene cation (Figure 4a, configurations 7 and 8). Similarly, the direct product of the first excited state of the pentacene cation and the ground state of the C_{60} anion represents the second excited charge transfer state (CT_2, Figure 4b, configurations 9−12).[48]

It is important to emphasize that the determinants shown in Figure 4 are not the true eigenfunctions of a many-electron Hamiltonian. They represent configurations known as diabatic states, which are often used for analysis of ET processes.[53,90−92] The true many-electron wave functions are linear combinations of such determinants. A rigorous solution for the multiconfigurational wave functions, for example, using a configuration interaction (CI) approach, is extremely demanding, especially for large systems. It is unlikely that a single ab initio electronic structure method can accurately describe all states involved in the photoinduced SF and ET processes even for fixed system geometry. Accurate description of the energies of the doubly excited configurations is not possible at the single-particle level. The energy of the ME state would be approximately twice as high as the energy of the S_1 state, while from the experiment it is known that their energies are nearly degenerate.[32,43] Lowering of the ME state energy with respect to the single-particle description originates from the electron−hole interactions. A direct ab initio electron−nuclear dynamics simulation involving accurate multiconfiguration wave functions extends beyond current computational capabilities.

To gain an understanding of the ET and SF dynamics coupled to nuclear motion, we consider a scheme based on the diabatic configurations shown in Figure 4. By grouping diabatic configurations of the same type (Figure 4), we achieve a certain degree of invariance with respect to the details of the true wave function composition. Even if the populations of individual configurations vary during the simulated dynamics, the sum of the populations of the diabatic states of a given type changes smoothly. This method of analysis allows us to approximate a computationally expensive dynamics based on CI-type wave function with a much more affordable simulation.

The average energy of each state used in the dynamics simulation is defined according to the experimental data. The nonadiabatic coupling between the states is obtained using the Slater determinant description,[49] because experimental data are not available for this purpose, while more rigorous computations are too demanding. The excitation energy of each configuration is derived from the differences in the KS orbital energies. The phonon-induced fluctuations in the energies of the KS orbitals are used to obtain the evolution of the state energies and nonadiabatic coupling. The average values of the state energies are shown in Figure 6a, along with a typical evolution of their instantaneous values during a short piece of the MD trajectory (Figure 6b). The shaded areas in Figure 6a represent the phonon-induced fluctuations of the state energies obtained during the MD.

The energy of the S_1 state is known from various sources, both experimental and theoretical. Zimmerman et al. computed values ranging from 2.08 eV[43] to 2.26 eV[44] for the pentacene monomer in the gas phase. Calculations in the crystalline phase show the Davydov energy levels at 1.73, 1.86, 2.13, and 2.27 eV.[55] Rao et al. report the Davydov levels of the S_1 state in the crystal phase positioned at 1.83 and 1.96 eV.[45] In addition, sidebands are observed at 2.02 and 2.21 eV. The value of 1.83 eV is also reported by a number of other authors.[40,46,47,56] In our model, the average energy of the S_1 state is set to 1.96 eV, making the average value of the lower-energy configuration 1 (Figure 4a) equal to 1.83 eV, according to the experimental data.

The energy of the ME state in pentacene is close to the energy of the S_1 state.[32,43] We set the average energy of the ME state to 1.96 eV, making it energetically resonant with the S_1 state (Figure 6a). The energy of the lowest configuration in the ME configuration manifold is close to 1.81 eV, in agreement with experiment.[32,43] The energy of the coupled triplet pair localized on the pentacene fragments is known to lie 0.11 eV below the energy level of the ME state.[32,40,43,45] Thus, in our model the average energy of this state is set equal to 1.85 eV.

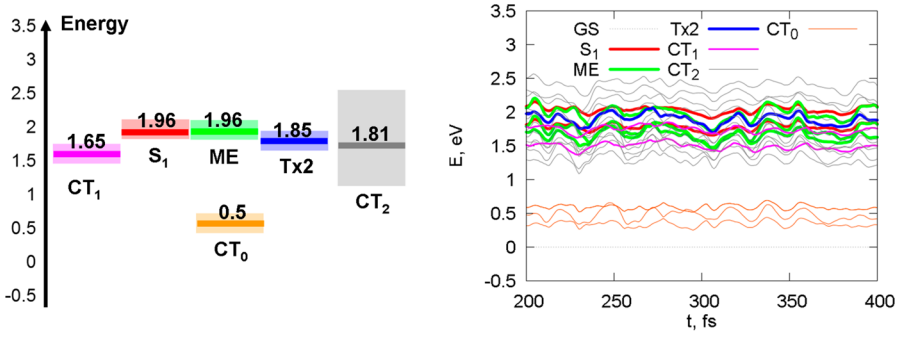

Figure 6. Energies of the key electronic states participating in the charge transfer and singlet fission dynamics in the pentacene/C_{60} system. (a) The average values and the range of fluctuations of the state energies. (b) Typical evolution of the state energies along a 200 fs piece of the MD trajectory.

dx.doi.org/10.1021/ja411800n | J. Am. Chem. Soc. 2014, 136, 1599−1608

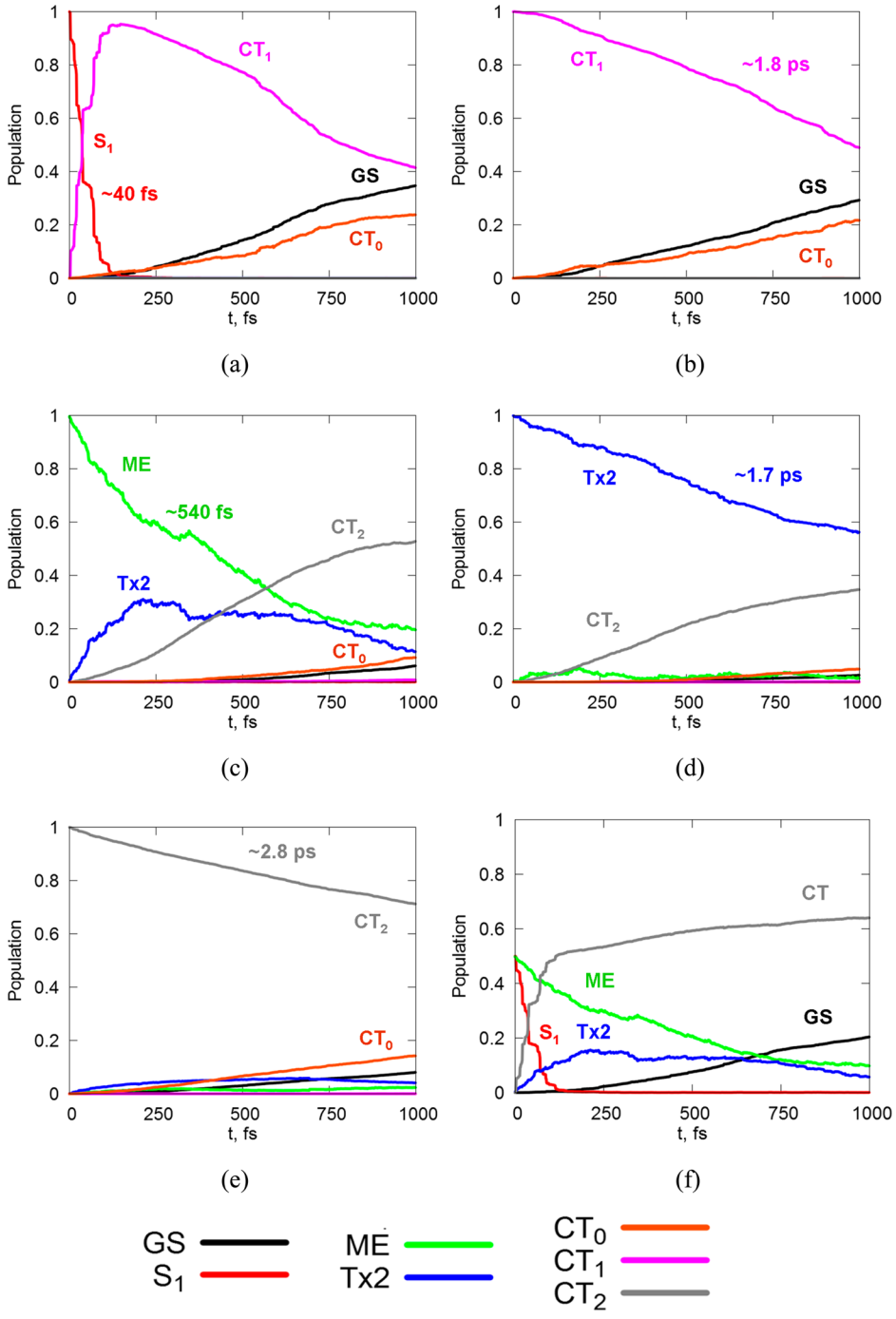

Figure 7. Relaxation dynamics of the key states involved in the singlet fission and charge transfer processes. Different panels represent different initial conditions. Panels a–e show dynamics starting from the S_1, CT_1, ME, Tx2, and CT_2 states, respectively. The dynamics shown in panel f starts from a superposition state with equal contributions of the ME and S_1 configurations. CT in panel (f) denotes the total population on the CT_0, CT_1, and CT_2 states.

The energy of the lowest charge transfer state (CT_0) is available from the experimental studies of Rao et al.[45] They estimate it as 0.5 eV, in agreement with the open-circuit voltage V_{oc} of 0.4 eV observed in pentacene/C_{60} solar cells.[45] The energy of this state is significantly affected by the Coulomb stabilization, as discussed by Yi et al.[48] The energy of the next two charge transfer states (CT_1 and CT_2) can be estimated by the energy difference with respect to the CT_0 state. The values have been reported experimentally, 1.15 eV[57] and 1.31 eV,[58] respectively. These relative estimates together with the 0.5 eV energy of the CT_0 state give the average energies of the CT_1 and CT_2 states at 1.65 and 1.85 eV, respectively. Because the LUMO of C_{60} is composed of three quasi-degenerate levels, and because the degeneracy is lifted by the environment and by the nuclear fluctuations, the configurations corresponding to the CT_2 state span a relatively wide energy window, as shown in Figure 6a. Because the minimum edge of this energy window is lower than the energy of the Tx2 and ME states, the charge transfer process is energetically favorable. A similar conclusion holds for the CT_1 and S_1 states: the transition from S_1 to CT_1 is

dx.doi.org/10.1021/ja411800n | J. Am. Chem. Soc. 2014, 136, 1599–1608

also energetically favorable. The S_1 state is directly coupled to the CT_1 state, but not to the CT_2 state (Figure 4). Similarly, the ME and Tx2 states are directly coupled to the CT_2 state, but not to the CT_1 state.

3.3. Relaxation and Charge Transfer Dynamics. To study the dynamics of state transformations, we calculate the populations of all states as functions of time, starting from different initial conditions. We consider only nonadiabatic transitions. Resonant energy transfer, a virtual two-photon process, provides an alternative mechanism. Described by the second-order time-dependent perturbation theory,[93] it happens on a nanosecond time scale,[94,95] and can be neglected for the studied sub-10 ps dynamics. Because the nature of the initial photoexcited state in the pentacene/C_{60} system remains a matter of debate,[32,40,42,44,47,56] each initial condition represents a different photoexcitation scenario. For instance, the traditional assumption that absorption of a photon populates the S_1 state has been augmented with the notions that the initial state may contain a superposition of the S_1 and ME states,[32] and that the photoexcited state can contain significant charge transfer character.[78] Panels a−e of Figure 7 represent the dynamics starting from the S_1, ME, Tx2, CT_1, and CT_2 states. Figure 7f considers the case in which the initial state of the system is prepared as a superposition of the S_1 and ME states with equal weights. The lifetime of each initial state is obtained from a single exponential fit, $P_I(t) = \exp(-(t/t_I))$.

The decay of the S_1 state happens on a very fast time scale of about 40 fs. The majority of the population goes into the CT_1 state (Figure 7a). The relaxation rate is in good agreement with the experimental and theoretical predictions of 70−100 fs.[32,42−44,56] It is important to note that relaxation of S_1 practically does not populate the ME state, nor does it populate the Tx2 state. This result arises because of very small nonadiabatic coupling between these pairs of states, although single particle selection rules allow such transitions. The result is in good agreement with the recent experimental observations of Chan et al.,[32] showing that the creation of the ME state does not stem from the decay of the S_1 state, and therefore the direct $S_1 \rightarrow$ Tx2 mechanism of SF is unlikely. Transitions between the S_1 and ME configurations are allowed; however, the small magnitude of the nonadiabatic coupling effectively shuts this pathway. It should be noted that the states may be coupled during the photoexcitation process, and the ME configurations may be populated by a laser pulse via the S_1 configurations. In this case, the coupling is realized via a transition dipole moment, which can be larger than the nonadiabatic coupling, opening the pathway for the duration of the laser pulse. This scenario is analogous to the photoexcitation mechanism of MEG in semiconductor quantum dots.[19,96]

Ab initio calculations indicate that the photoexcited state of the systems undergoing SF can have substantial charge transfer character,[78] motivating us to study the dynamics starting from the CT configurations. In contrast to the relaxation of the S_1 state, the CT_1 state decays on a significantly longer time scale of 1.8 ps (Figure 7b). The majority of the population goes to the lower-energy charge transfer state CT_0. In turn, the CT_0 state relaxes to the ground state (GS) on a 750 fs time scale. Both S_1 and CT_1 states may relax to the GS directly, but this process is very slow, because of small nonadiabatic couplings.

The ME state relaxes within 540 fs, populating the Tx2 state on a 240 fs time scale (Figure 7c). The Tx2 state is populated only transiently, because it is energetically higher than the CT_2 state and is coupled to it. Because the relaxation of Tx2 down to CT_2 happens on the 1.7 ps time scale that is longer than the time of transition from ME to Tx2, the population of the Tx2 state reaches a saturation level at about 33% and then decreases. The decay of Tx2 to the CT_2 state is favorable for the photovoltaic effect. It shows that if the pentacene subsystem is coupled to the fullerene layer, the SF process is followed immediately by charge separation. Note that the Tx2 state considered in our model is not a fully dissociated pair of triplets. Rather, it is an intermediate having the coupled triplet character. The relatively fast Tx2→CT_2 transition may account for the quenching of the slow transitions observed by Thorsmolle et al.[46,47]

The rise time of the Tx2 state, estimated as 240 fs, falls in the middle of the experimental range. Jundt et al.[56] and Wilson et al.[42] report 80 fs, while Chan et al. estimate a 900 fs time scale.[32] It should be noted that the interpretation of the SF process performed by Jundt and Wilson involved no ME state. The observed time may correspond more closely to exciton delocalization rather than to electronic transitions between different types of states. In comparison, Chan et al. consider SF to occur by an electronic transition between the ME and Tx2 states. Similarly to Chan et al., we associate the SF time with the appearance of the Tx2 state. Tx2 does not arise directly from the S_1 state. Rather, it stems from the ME state. This emphasizes the crucial role the ME state plays in the SF process, supporting the earlier puiblications.[32,43]

Transfer of population from the ME state to the CT_2 state starts once the population of the Tx2 state has reached a steady-state saturation level at ∼240 fs. Because the relaxation of the Tx2 state is relatively slow (∼1.7 ps, Figure 7d), the following rise of the CT_2 state can be approximately attributed to the decay of the ME state. Thus, the rise time of CT_2 state due to decay of ME can be estimated as 540 − 240 = 300 fs. This rate is in good agreement with the experimental data by Chan et al.,[32] who reports a value of ca. 400 ± 100 fs.

The Tx2 and CT_2 states relax on the relatively slow time scales of ∼1.7 and ∼2.8 ps, giving rise to CT_2 and CT_0, respectively (Figure 7d,e). The decay time of the Tx2 state is also reported by Chan et al.[32] who estimated it as ca. 5 ps. It should be noted that in our simulations Tx2 → CT_2 and CT_2 → CT_0 are one-electron transfer processes. The complete two-electron transfer process Tx2 → CT_0 would then require 1.7 + 2.8 = 4.5 ps, in excellent agreement with the reported experimental value.

Excitation of a superposition of the S_1 and ME states leads to charger transfer from the pentacene crystal to the C_{60} layer, providing direct computational evidence of the photovoltaic effect in the combined system, in agreement with experiment.[32,45] The Tx2 state is populated transiently and survives on a picosecond time scale, also in agreement with experiment.[32] Our simulations show that photoexcitation of a state with ME character is essential for SF. Tx2 decays fairly rapidly into a CT state, after which a second CT step takes place on a slower time scale, in competition with charge diffusion in a layered pentacene/C_{60} system. The exact nature of the photoexcitation in the pentacene crystal necessitates an explicit treatment of light-matter interaction. The photoexcited state may depend on whether one uses a short laser pulse, as in pump−probe experiments, or a continuous-wave radiation, as expected under sunlight conditions.

3.4. Overall Kinetic Scheme. As we have shown in the previous sections, the constructed model allows us to describe kinetics of various quantum transitions involved in the SF,

dx.doi.org/10.1021/ja411800n | J. Am. Chem. Soc. 2014, 136, 1599−1608

charge transfer, and nonradiative relaxation processes, and to obtain time scales that are in good agreement with the experimental measurements. The overall kinetic scheme is summarized in Figure 8. Because not all experimental and

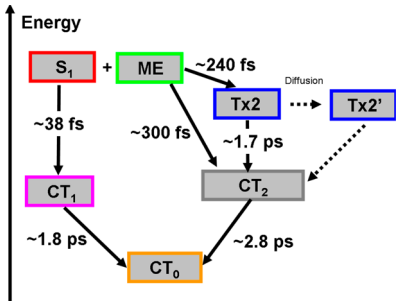

Figure 8. A comprehensive kinetic scheme of the population and ET steps involved in the SF and charge separation processes at the pentacene/C_{60} interface.

theoretical results are in agreement with each other, it is important to build a consistent theoretical framework for the description of the photoinduced dynamics. In this section, we discuss the constraints implied by our model and relate the model to the existing data.

The available experimental and theoretical results provide mixed information on the states involved in the SF and charge transfer processes in the pentacene/C_{60} system, and on the alignment of the state energies with respect to each other. In particular, if the CT_0 state is assumed to be positioned at 1.3 eV with respect to the GS level, as proposed by Yi et al.,[48] the CT_1 and CT_2 states become too high in energy and do not play any significant role in the charge separation. This would imply that the only possibility for the ME state to be involved in the charge transfer would be to relax to the CT_0 state directly. Such direct transition is prohibited at the single-particle level, because it involves simultaneous transfer of two electrons. To be allowed, the process should involve intermediate configurations of the CT_2 character. If the latter were higher in energy than the ME state, the rate would be very slow. In experiment, however, the rise of the CT state population due to ME decay happens on a relatively fast time scale of ~400 fs.[32]

To explain the experiments by Chan et al.[32] on the ME decay, it is necessary to assume that the energy of the CT_0 state is in the 0.5 eV range, as estimated by Rao et al.[45] In such a case, both CT_1 and CT_2 states are located below ME and S_1 on the energy scale. This allows the ME state to relax to CT_2 and then to CT_0 from both thermodynamic and kinetic points of view. Such a supposition also predicts that the S_1 state relaxes down to the CT_1 state. This result agrees with the ultrafast quenching of the SF channel by the C_{60} dopant in pentacene crystals, observed by Thorsmolle et al.[46,47] The energy of the resulting charge transfer state reported in this spectroscopic study is estimated to be ~1.9 eV, in good comparison with the energy of the CT_1 state in present work (~1.65 eV).

Our quantum-chemical calculations show that the nonadiabatic coupling between the S_1 and ME states is relatively small. Thus, the main channel of decay of the S_1 configuration is to the CT_1 state. It is important to note that if the coupling were large, the S_1 and ME states would reach an equilibrium with each other, which would effectively slow the S_1 state relaxation. The nonadiabatic coupling between the S_1 state and the GS is also small. As a result, the nonradiative decay of the S_1 state to the GS is slow, and the fluorescence of the S_1 state is long-lived, many picoseconds, in good agreement with the experimental knowledge.[32,40,43,45−47,56−58]

4. CONCLUSIONS

We constructed a minimalistic model for a time-domain atomistic description of the charge transfer and SF processes in the pentacene/C_{60} solar cell. The model unifies the available experimental and theoretical data, helping to resolve inconsistent results regarding the nature and importance of intermediate states, energy level alignment, SF mechanism, and time scales of quantum dynamics. The model emphasizes the importance of various intermediate states. In particular, several pentacene−pentacene and pentacene−fullerene charge transfer configurations should be taken into account to explain the observable charge and energy transfer times. SF in the pentacene layer is mediated by configurations with charge transfer between different pentacene molecules. These configurations can be viewed as either independent states, or components of the ME and Tx2 states arising due to electron correlation effects. The dynamics in the system combining the pentacene and C_{60} layers involves several charge transfer states with the electron localized on C_{60} and the hole remaining on pentacene.

The relative energies of the states involved in the photoinduced dynamics should be carefully aligned with respect to each other, as in Figure 6, to describe the measured time scales. Assigning the energy of the CT_0 state around 0.5 eV, as in the experiment of Rao et al.,[45] produces a consistent quantum dynamical scheme. An interesting way of controlling the SF efficiency can be suggested on the basis of the energy alignment. If the CT_2 state in the heterojunction system is designed to have the energy larger than that of the Tx2 state, triplet production can be maximized. After dissociation of the triplet pair, each triplet can access states of the CT_0 type, provided that their energy is lower than the energy of the Tx2 state. The generation of two electron−hole pairs then will be maximized.

By testing other possible models, different in either the type of intermediate configurations or the state energies, we found that alternative schemes break down at a certain point, failing to explain some of the discussed facts. Despite its simplicity and approximations used, our scheme is capable of predicting the electronic transition times for the key processes involved, from the photoexcitation to the final charge separation, in good agreement with the existing experimental data.

The S_1 and ME states involved in the SF process are coupled rather weakly. Direct nonadiabatic transitions between these states are suppressed, although not forbidden. Because the S_1 and Tx2 states are also weakly coupled, the triplet production originates only from the ME state, which is populated during photoexcitation. Generally, photoexcitation creates a superposition of the S_1 and ME configurations. To maximize the SF yield, one should design systems and utilize photoexcitation conditions, under which the contribution of the ME configurations is maximized. One can also consider designing electromagnetic fields to directionally pump the S_1 state into ME or Tx2.

Our model makes no assumptions regarding separation of time scales for the competing processes and about particular types of kinetics, for example, exponential or Gaussians. This emphasizes the robustness of the methodology and its ab initio nature. At the same time, the use of the experimental data for

specifying the state energies adds a semiempirical flavor. The model provides a fully atomistic description of the photo-induced dynamics, including simultaneously electronic and nuclear evolutions. The reported analysis enhances understanding of the complex quantum dynamics in nanoscale materials capable of the SF and charge transfer processes.

AUTHOR INFORMATION

Corresponding Author

oleg.prezhdo@rochester.edu

Notes

The authors declare no competing financial interest.

ACKNOWLEDGMENTS

We are grateful to Drs. Heather Jaeger and Lin Jun Wang for useful discussions and comments, and acknowledge financial support from the National Science Foundation, grant CHE-1050405.

REFERENCES

(1) Walter, M. G.; Warren, E. L.; McKone, J. R.; Boettcher, S. W.; Mi, Q.; Santori, E. A.; Lewis, N. S. *Chem. Rev.* **2010**, *110*, 6446−6473.
(2) Hagfeldt, A.; Boschloo, G.; Sun, L.; Kloo, L.; Pettersson, H. *Chem. Rev.* **2010**, *110*, 6595−6663.
(3) Kubacka, A.; Fernández-García, M.; Colón, G. *Chem. Rev.* **2012**, *112*, 1555−1614.
(4) Akimov, A. V.; Neukirch, A. J.; Prezhdo, O. V. *Chem. Rev.* **2013**, *113*, 4496.
(5) Barber, G. D.; Hoertz, P. G.; Lee, S. H. A.; Abrams, N. M.; Mikulca, J.; Mallouk, T. E.; Liska, P.; Zakeeruddin, S. M.; Grätzel, M.; Ho-Baillie, A.. *J. Phys. Chem. Lett.* **2010**, *2*, 581−585.
(6) Johnson, J. C.; Nozik, A. J.; Michl, J. *J. Am. Chem. Soc.* **2010**, *132*, 16302−16303.
(7) Kim, D. R.; Lee, C. H.; Rao, P. M.; Cho, I. S.; Zheng, X. L. *Nano Lett.* **2011**, *11*, 2704−2708.
(8) Barea, E. M.; Shalom, M.; Giménez, S.; Hod, I.; Mora-Seró, I.; Zaban, A.; Bisquert, J. *J. Am. Chem. Soc.* **2010**, *132*, 6834−6839.
(9) Zhu, J.; Hsu, C.-M.; Yu, Z.; Fan, S.; Cui, Y. *Nano Lett.* **2010**, *10*, 1979−1984.
(10) Lee, J.; Vandewal, K.; Yost, S. R.; Bahlke, M. E.; Goris, L.; Baldo, M. A.; Manca, J. V.; Voorhis, T. V. *J. Am. Chem. Soc.* **2010**, *132*, 11878−11880.
(11) Chan, W.-L.; Tritsch, J. R.; Zhu, X.-Y. *J. Am. Chem. Soc.* **2012**, *134*, 18295−18302.
(12) Musser, A. J.; Al-Hashimi, M.; Maiuri, M.; Brida, D.; Heeney, M.; Cerullo, G.; Friend, R. H.; Clark, J. *J. Am. Chem. Soc.* **2013**, *135*, 12747−12754.
(13) Paci, I.; Johnson, J. C.; Chen, X.; Rana, G.; Popovic, D.; David, D. E.; Nozik, A. J.; Ratner, M. A.; Michl, J. *J. Am. Chem. Soc.* **2006**, *128*, 16546−16553.
(14) Difley, S.; Van Voorhis, T. *J. Chem. Theory Comput.* **2011**, *7*, 594−601.
(15) Xiao, D.; Martini, L. A.; Snoeberger, R. C.; Crabtree, R. H.; Batista, V. S. *J. Am. Chem. Soc.* **2011**, *133*, 9014−9022.
(16) Sánchez-de-Armas, R.; Oviedo López, J.; A. San-Miguel, M.; Sanz, J. F.; Ordejón, P.; Pruneda, M. *J. Chem. Theory Comput.* **2010**, *6*, 2856−2865.
(17) Kilin, D. S.; Pereversev, Y. V.; Prezhdo, O. V. *J. Chem. Phys.* **2004**, *120*, 11209.
(18) Kilina, S. V.; Craig, C. F.; Kilin, D. S.; Prezhdo, O. V. *J. Phys. Chem. C* **2007**, *111*, 4871−4878.
(19) Fischer, S. A.; Madrid, A. B.; Isborn, C. M.; Prezhdo, O. V. *J. Phys. Chem. Lett.* **2009**, *1*, 232−237.
(20) Fischer, S. A.; Isborn, C. M.; Prezhdo, O. V. *Chem. Sci.* **2011**, *2*, 400.
(21) Hyeon-Deuk, K.; Prezhdo, O. V. *Nano Lett.* **2011**, *11*, 1845−1850.
(22) Isborn, C. M.; Kilina, S. V.; Li, X.; Prezhdo, O. V. *J. Phys. Chem. C* **2008**, *112*, 18291−18294.
(23) Fischer, S. A.; Duncan, W. R.; Prezhdo, O. V. *J. Am. Chem. Soc.* **2009**, *131*, 15483−15491.
(24) Yost, S. R.; Wang, L.-P.; Van Voorhis, T. *J. Phys. Chem. C* **2011**, *115*, 14431−14436.
(25) Shockley, W.; Queisser, H. J. *J. Appl. Phys.* **1961**, *32*, 510.
(26) Kolodinski, S.; Werner, J. H.; Wittchen, T.; Queisser, H. J. *Appl. Phys. Lett.* **1993**, *63*, 2405.
(27) Christensen, O. *J. Appl. Phys.* **1976**, *47*, 689.
(28) Cunningham, P. D.; Boercker, J. E.; Foos, E. E.; Lumb, M. P.; Smith, A. R.; Tischler, J. G.; Melinger, J. S. *Nano Lett.* **2011**, *11*, 3476−3481.
(29) Wang, S.; Khafizov, M.; Tu, X.; Zheng, M.; Krauss, T. D. *Nano Lett.* **2010**, *10*, 2381−2386.
(30) Styers-Barnett, D. J.; Ellison, S. P.; Mehl, B. P.; Westlake, B. C.; House, R. L.; Park, C.; Wise, K. E.; Papanikolas, J. M. *J. Phys. Chem. C* **2008**, *112*, 4507−4516.
(31) Bange, S.; Scherf, U.; Lupton, J. M. *J. Am. Chem. Soc.* **2012**, *134*, 1946−1949.
(32) Chan, W.-L.; Ligges, M.; Jailaubekov, A.; Kaake, L.; Miaja-Avila, L.; Zhu, X.-Y. *Science* **2011**, *334*, 1541−1545.
(33) Greyson, E. C.; Vura-Weis, J.; Michl, J.; Ratner, M. A. *J. Phys. Chem. B* **2010**, *114*, 14168−14177.
(34) Jadhav, P. J.; Mohanty, A.; Sussman, J.; Lee, J.; Baldo, M. A. *Nano Lett.* **2011**, *11*, 1495−1498.
(35) Marciniak, H.; Fiebig, M.; Huth, M.; Schiefer, S.; Nickel, B.; Selmaier, F.; Lochbrunner, S. *Phys. Rev. Lett.* **2007**, *99*, 176402.
(36) Marciniak, H.; Pugliesi, I.; Nickel, B.; Lochbrunner, S. *Phys. Rev. B* **2009**, 79.
(37) Minami, T.; Nakano, M. *J. Phys. Chem. Lett.* **2011**, *3*, 145−150.
(38) Muntwiler, M.; Yang, Q.; Zhu, X.-Y. *J. Electron Spectrosc. Relat. Phenom.* **2009**, *174*, 116−124.
(39) Roberts, S. T.; McAnally, R. E.; Mastron, J. N.; Webber, D. H.; Whited, M. T.; Brutchey, R. L.; Thompson, M. E.; Bradforth, S. E. *J. Am. Chem. Soc.* **2012**, *134*, 6388−6400.
(40) Smith, M. B.; Michl, J. *Chem. Rev.* **2010**, *110*, 6891−6936.
(41) Wang, C.; Tauber, M. J. *J. Am. Chem. Soc.* **2010**, *132*, 13988−13991.
(42) Wilson, M. W. B.; Rao, A.; Clark, J.; Kumar, R. S. S.; Brida, D.; Cerullo, G.; Friend, R. H. *J. Am. Chem. Soc.* **2011**, *133*, 11830−11833.
(43) Zimmerman, P. M.; Zhang, Z.; Musgrave, C. B. *Nature* **2010**, *2*, 648−652.
(44) Zimmerman, P. M.; Bell, F.; Casanova, D.; Head-Gordon, M. *J. Am. Chem. Soc.* **2011**, *133*, 19944−19952.
(45) Rao, A.; Wilson, M. W. B.; Hodgkiss, J. M.; Albert-Seifried, S.; Bassler, H.; Friend, R. H. *J. Am. Chem. Soc.* **2010**, *132*, 12698−12703.
(46) Thorsmølle, V. K.; Averitt, R. D.; Demsar, J.; Smith, D. L.; Tretiak, S.; Martin, R. L.; Chi, X.; Crone, B. K.; Ramirez, A. P.; Taylor, A. J. *Phys. Rev. Lett.* **2009**, *102*, 17401.
(47) Thorsmølle, V. K.; Averitt, R. D.; Demsar, J.; Smith, D. L.; Tretiak, S.; Martin, R. L.; Chi, X.; Crone, B. K.; Ramirez, A. P.; Taylor, A. J. *Physica B* **2009**, *404*, 3127−3130.
(48) Yi, Y.; Coropceanu, V.; Brédas, J.-L *J. Am. Chem. Soc.* **2009**, *131*, 15777−15783.
(49) Craig, C.; Duncan, W.; Prezhdo, O. *Phys. Rev. Lett.* **2005**, *95*, 163001.
(50) Duncan, W. R.; Craig, C. F.; Prezhdo, O. V. *J. Am. Chem. Soc.* **2007**, *129*, 8528−8543.
(51) Fischer, S. A.; Habenicht, B. F.; Madrid, A. B.; Duncan, W. R.; Prezhdo, O. V. *J. Chem. Phys.* **2011**, *134*, 24102.
(52) Hyeon-Deuk, K.; Prezhdo, O. V. *ACS Nano* **2012**, *6*, 1239−1250.
(53) Tully, J. C. *J. Chem. Phys.* **1990**, *93*, 1061−1071.
(54) Sholl, D. S.; Tully, J. C. *J. Chem. Phys.* **1998**, *109*, 7702.
(55) Tiago, M.; Northrup, J.; Louie, S. *Phys. Rev. B* **2003**, *67*, 115212.
(56) Jundt, C.; Klein, G.; Sipp, B.; Le Moigne, J.; Joucla, M.; Villaeys, A. A. *Chem. Phys. Lett.* **1995**, *241*, 84−88.

(57) Kato, T.; Kodama, T.; Shida, T.; Nakagawa, T.; Matsui, Y.; Suzuki, S.; Shiromaru, H.; Yamauchi, K.; Achiba, Y. *Chem. Phys. Lett.* **1991**, *180*, 446−450.
(58) Szczepanski, J.; Wehlburg, C.; Vala, M. *Chem. Phys. Lett.* **1995**, *232*, 221−228.
(59) Gianozzi, P.; Baroni, S.; Bonini, N.; Calandra, M.; Car, R.; Cavazzoni, C.; Ceresoli, D.; Chiarotti, G. L.; Cococcioni, M.; Dabo, I.; Dal Corso, A.; de Gironcoli, S.; Fabris, S.; Fratesi, G.; Gebauer, R.; Gerstmann, U.; Gougoussis, C.; Kokalj, A.; Lazzeri, M.; Martin-Samos, L.; Marzari, N.; Mauri, F.; Mazzarello, R.; Paolini, S.; Pasquarello, A.; Paulatto, L.; Sbraccia, C.; Scandolo, S.; Sclauzero, G.; Seitsonen, A. P.; Smogunov, A.; Umari, P.; Wentzcovitch, R. M. *J. Phys.: Condens. Matter* **2009**, *21*, 395592.
(60) Perdew, J. P.; Burke, K.; Ernzerhof, M. *Phys. Rev. Lett.* **1996**, *77*, 3865−3868.
(61) Perdew, J. P.; Burke, K. *Phys. Rev. Lett.* **1997**, *78*, 1396.
(62) Barone, V.; Casarin, M.; Forrer, D.; Pavone, M.; Sambi, M.; Vittadini, A. *J. Comput. Chem.* **2009**, *30*, 934−939.
(63) Grimme, S. *J. Comput. Chem.* **2006**, *27*, 1787−1799.
(64) Muccioli, L.; D'Avino, G.; Zannoni, C. *Adv. Mater.* **2011**, *23*, 4532−4536.
(65) Nose, S. A *J. Chem. Phys.* **1984**, *81*, 511−519.
(66) Nose, S. *J. Phys. Soc. Jpn.* **2001**, *70*, 75−77.
(67) Hoover, W. G. *Mol. Simul.* **2007**, *33*, 13.
(68) Hoover, W. G. *Phys. Rev. A* **1989**, *40*, 2814−2815.
(69) Akimov, A. V.; Prezhdo, O. V. *J. Chem. Theory Comput.* **2013**, *9*, 4959−4972.
(70) Fabiano, E.; Keal, T. W.; Thiel, W. *Chem. Phys.* **2008**, *349*, 334−347.
(71) Prezhdo, O. V.; Duncan, W. R.; Prezhdo, V. V. *Prog. Surf. Sci.* **2009**, *84*, 30−68.
(72) Hack, M. D.; Truhlar, D. G. *J. Phys. Chem. A* **2000**, *104*, 7917−7926.
(73) Hack, M. D.; Wensmann, A. M.; Truhlar, D. G.; Ben-Nun, M.; Martínez, T. J. *J. Chem. Phys.* **2001**, *115*, 1172.
(74) Fabiano, E.; Groenhof, G.; Thiel, W. *Chem. Phys.* **2008**, *351*, 111−116.
(75) Nelson, T.; Fernandez-Alberti, S.; Chernyak, V.; Roitberg, A. E.; Tretiak, S. *J. Phys. Chem. B* **2011**, *115*, 5402−5414.
(76) Nelson, T.; Fernandez-Alberti, S.; Chernyak, V.; Roitberg, A. E.; Tretiak, S. *J. Chem. Phys.* **2012**, *136*, 054108.
(77) Hammes-Schiffer, S.; Tully, J. C. *J. Chem. Phys.* **1994**, *101*, 4657.
(78) Sharifzadeh, S.; Darancet, P.; Kronik, L.; Neaton, J. B. *J. Phys. Chem. Lett.* **2013**, *4*, 2197−2201.
(79) Kilina, S. V.; Neukirch, A. J.; Habenicht, B. F.; Kilin, D. S.; Prezhdo, O. V. *Phys. Rev. Lett.* **2013**, *110*, 180404.
(80) Long, R.; Prezhdo, O. V. *J. Am. Chem. Soc.* **2011**, *133*, 19240−19249.
(81) Long, R.; English, N. J.; Prezhdo, O. V. *J. Am. Chem. Soc.* **2012**, *134*, 14238−14248.
(82) Akimov, A. V.; Muckerman, J. T.; Prezhdo, O. V. *J. Am. Chem. Soc.* **2013**, *135*, 8682.
(83) Müller, A. M.; Avlasevich, Y. S.; Schoeller, W. W.; Müllen, K.; Bardeen, C. J. *J. Am. Chem. Soc.* **2007**, *129*, 14240−14250.
(84) Godby, R. W.; Schlüter, M.; Sham, L. J. *Phys. Rev. B* **1988**, *37*, 10159.
(85) Gygi, F.; Baldereschi, A. *Phys. Rev. Lett.* **1989**, *62*, 2160−2163.
(86) Levine, Z. H.; Allan, D. C. *Phys. Rev. Lett.* **1989**, *63*, 1719−1722.
(87) Finazzi, E.; Di Valentin, C.; Pacchioni, G.; Selloni, A. *J. Chem. Phys.* **2008**, *129*, 154113.
(88) Hybertsen, M. S.; Louie, S. G. *Phys. Rev. Lett.* **1985**, *55*, 1418−1421.
(89) Hybertsen, M. S.; Louie, S. G. *Phys. Rev. B* **1986**, *34*, 5390.
(90) Marcus, R. A. *Annu. Rev. Phys. Chem.* **1964**, *15*, 155−196.
(91) Hammes-Schiffer, S.; Stuchebrukhov, A. A. *Chem. Rev.* **2010**, *110*, 6939−6960.
(92) Roy, S.; Shenvi, N. A.; Tully, J. C. *J. Chem. Phys.* **2009**, *130*, 174716.
(93) Andrews, D. L. A. *Chem. Phys.* **1989**, *135*, 195−201.
(94) Kilin, D. S.; Tsemekhman, K.; Prezhdo, O. V.; Zenkevich, E. I.; von Borczyskowski, C. *J. Photochem. Photobiol., A* **2007**, *190*, 342−351.
(95) Kilin, D. S.; Tsemekhman, K. L.; Kilina, S. V.; Balatsky, A. V.; Prezhdo, O. V. *J. Phys. Chem. A* **2009**, *113*, 4549−4556.
(96) Isborn, C. M.; Kilina, S. V.; Li, X.; Prezhdo, O. V. *J. Phys. Chem. C* **2008**, *112*, 18291−18294.